



## **Optimization of Sea Surface Current Retrieval Using a Maximum Cross-Correlation Technique on Modeled Sea Surface Temperature**

Downloaded from: <https://research.chalmers.se>, 2025-12-06 04:17 UTC

Citation for the original published paper (version of record):

Heuzé, C., Carvajal, G., Eriksson, L. (2017). Optimization of Sea Surface Current Retrieval Using a Maximum Cross-Correlation Technique on Modeled Sea Surface Temperature. *Journal of Atmospheric and Oceanic Technology*, 34(10): 2245-2255. <http://dx.doi.org/10.1175/jtech-d-17-0029.1>

N.B. When citing this work, cite the original published paper.

## Optimization of Sea Surface Current Retrieval Using a Maximum Cross-Correlation Technique on Modeled Sea Surface Temperature

CÉLINE HEUZÉ

*Department of Marine Sciences, University of Gothenburg, Gothenburg, Sweden*

GISELA K. CARVAJAL AND LEIF E. B. ERIKSSON

*Department of Space, Earth and Environment, Chalmers University of Technology, Gothenburg, Sweden*

(Manuscript received 15 February 2017, in final form 22 July 2017)

### ABSTRACT


Using sea surface temperature from satellite images to retrieve sea surface currents is not a new idea, but so far its operational near-real-time implementation has not been possible. Validation studies are too region specific or uncertain, sometimes because of the satellite images themselves. Moreover, the sensitivity of the most common retrieval method, the maximum cross correlation, to the parameters that have to be set is unknown. Using model outputs instead of satellite images, biases induced by this method are assessed here, for four different seas of western Europe, and the best of nine settings and eight temporal resolutions are determined. The regions with strong currents return the most accurate results when tracking a 20-km pattern between two images separated by 6–9 h. The regions with weak currents favor a smaller pattern and a shorter time interval, although their main problem is not inaccurate results but missing results: where the velocity is too low to be picked by the retrieval. The results are not impaired by the restrictions imposed by ocean surface current dynamics and available satellite technology, indicating that automated sea surface current retrieval from sea surface temperature images is feasible, for pollution confinement, search and rescue, and even for more energy-efficient and comfortable ship navigation.

### 1. Introduction

Knowledge about near-real-time ocean surface currents is essential to many commercial and societal sectors. These include, for example, life-saving search and rescue missions and oil spill confinement (Klemas 2012), but also navigation planning to reduce fuel consumption (Ronen 2011). Close to the coast, ocean surface currents can be measured by ground-based radars (Stewart and Joy 1974), but no such facilities exist in the open ocean. Furthermore, altimetry products are available only as daily 25–50-km grids (e.g., Pascual et al. 2007), which is not a high enough resolution for this type of applications.

Sea surface temperature (SST) in contrast is measured globally every 2–6 h by Advanced Very High Resolution Radiometer (AVHRR) instruments, at 1-km horizontal resolution, hence 30 years ago the idea of using SST to infer sea surface currents emerged. Emery et al. (1986) were the first to use the maximum cross-correlation (MCC) method for that purpose. Assuming that SST patterns are solely advected, this method tracks patterns that are most correlated between two consecutive satellite images and hence retrieves the current velocities by calculating the displacement of each pattern from one image to the next.

Since satellite images are affected by noise, clouds, geometric or geolocation mismatches, atmospheric distortion, etc., the validation of the MCC method is not straightforward and is better done with modeled sea

 Denotes content that is immediately available upon publication as open access.

Corresponding author: Céline Heuzé, celine.heuze@marine.gu.se



This article is licensed under a [Creative Commons Attribution 4.0 license](http://creativecommons.org/licenses/by/4.0/) (<http://creativecommons.org/licenses/by/4.0/>).

DOI: 10.1175/JTECH-D-17-0029.1

surface current and temperature fields. Tokmakian et al. (1990) and Wahl and Simpson (1990) notably used models to assess the time interval that is needed between two images for the advection assumption to be valid. Wahl and Simpson (1990) found that horizontal diffusion was negligible for time intervals smaller than 24 h, and both studies concluded that a time interval smaller than 12 h is necessary for local heating or cooling effects (Wahl and Simpson 1990) and vertical mixing (Tokmakian et al. 1990) to be negligible compared to advection. These and subsequent studies (e.g., Emery et al. 1992; Simpson and Gobat 1994; Marcello et al. 2008) however used relatively simplistic ocean circulation models, so Doronzo et al. (2015) checked the validity of the MCC method using a high-resolution (1 km) 3-hourly realistic model, the Regional Oceanic Modeling System (ROMS; Shchepetkin and McWilliams 2005). But this and all the previous studies all reach the same conclusion: their results may be region specific, so they prove only that the MCC applied to SST is effective at retrieving sea surface current over the limited area that they studied.

In this paper, we use high-resolution ocean analysis products from the Copernicus Marine Environment Monitoring Service, available every hour at a 2-km horizontal resolution, to validate the use of the MCC method applied to sea surface temperature over four different regions and to show that the validation is in fact not region specific. To the best of our knowledge, we also provide the first sensitivity study of the settings of the MCC method. The model and methods that we use are briefly described in section 2. The results are presented and discussed in section 3, focusing first on the sensitivity study and then on the possible inaccuracies caused by the specificities of each sea. We conclude on the limitations and feasibility of an operational use of this method in section 4.

## 2. Data and methods

We use four weeks of hourly  $0.03^\circ$  horizontal resolution (2 km) output from the Atlantic-Iberian Biscay Irish-Ocean Physics Analysis and Forecast system provided by the EU Copernicus Marine Environment Monitoring Service. This model is based on an eddy-resolving  $0.03^\circ$  application of the Nucleus for European Modelling of the Ocean (NEMO; Madec 2008), forced every 3 h by atmospheric fields from the European Centre for Medium-Range Weather Forecasts (ECMWF). For more information about this product and in particular its accuracy when compared with satellite imagery, the reader is referred to Sotillo et al. (2015). The outputs used here are the sea surface velocities  $u$  and  $v$ , and the

SST, in January, April, July, and October 2016, from 0000 UTC on the 21st of the month to 2300 UTC on the 27th of the month. These were last accessed on 6 April 2017. We divided the output into the four seas that it spans (from north to south):

- the North Sea,  $51^\circ$ – $56^\circ$ N,  $2.5^\circ$ W– $5^\circ$ E, covering a sea area of 165 000 km<sup>2</sup>;
- the Channel,  $48.5^\circ$ – $51^\circ$ N,  $6^\circ$ W– $2^\circ$ E, covering a sea area of 85 000 km<sup>2</sup>;
- the Bay of Biscay,  $43^\circ$ – $48^\circ$ N,  $6^\circ$ – $1^\circ$ W, covering a sea area of 160 000 km<sup>2</sup>;
- and the western Mediterranean Sea,  $36^\circ$ – $45^\circ$ N,  $1^\circ$ W– $5^\circ$ E, covering a sea area of 270 000 km<sup>2</sup>.

To retrieve the sea surface velocities from the sea surface temperature we use the MCC method (Emery et al. 1986). It consists of tracking features in SST between two images (here two time steps). The user defines the size of the pattern from the first image to track, as well as the largest area to look around in the second image. The displacement of the water corresponds to the distance between the location of the original pattern and the location of the pattern in the second image, which is most correlated to the original one. Three settings hence have to be chosen to apply the MCC method, whose sensitivity is seldom studied:

- the time interval between the two images (here considering only the images every 1 to 6, 9, and 12 h);
- the size of the template in the first image (here  $5 \times 5$ ,  $10 \times 10$ , or  $20 \times 20$  km);
- the size of the search area radius in the second image (here a radius of 10, 20, or 30 km around the template).

Hence in practice, the resolution of the retrieved velocity depends on the time interval and varies from  $0.55 \text{ m s}^{-1}$  for 1 h to  $0.05 \text{ m s}^{-1}$  for 12 h. To avoid any coastline effect, the algorithm as applied here does not consider the points within a search area of the coast and edges.

The comparison between the reference velocities, directly provided by the model, and the retrieved velocities, obtained by applying the MCC method, is made using two main methods. We first assess which percentage of the retrieved field that is returned is within  $0.2 \text{ m s}^{-1}$  (as done by, e.g., Bowen et al. 2002; Warren et al. 2016) and  $45^\circ$  in direction of the original field. In a real-life situation, this would give an indication of the size of the work area and ensure that it is in the correct sector.

We also use Taylor diagrams (Taylor 2001), a common method when comparing climate model simulations. These diagrams provide a visual representation of which method is the closest to the reference (here the

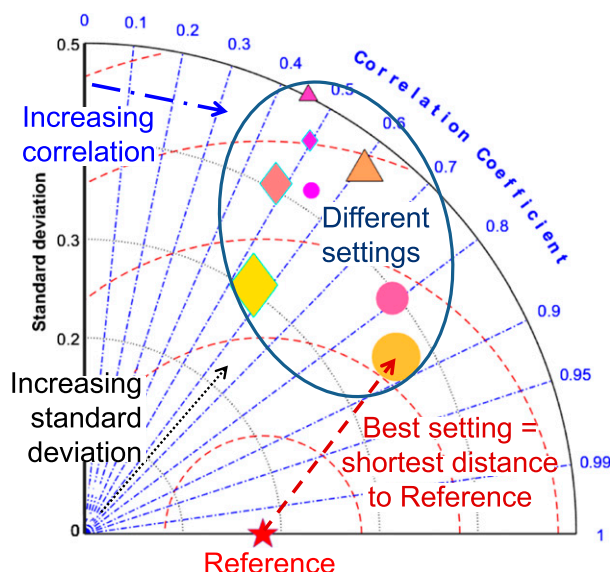


FIG. 1. A simplified explanation of a Taylor diagram (Taylor 2001). The reference (here, the velocity from the model) is on the x axis, and the best setting is the one whose symbol lies closest to the reference. The distance to the reference depends mostly on the correlation between the reference field and the retrieved velocities (blue lines) and the standard deviation of both fields (the black quarter circle; the value on the x axis for the reference and y axis for each setting).

original model velocity fields), as explained in Fig. 1. The best setting is the one with the highest temporal correlation to the reference field, the smallest RMS difference to it, and the closest standard deviation to that of the reference. We plot one Taylor diagram per time interval setting and per sea, hence showing on the same diagram the nine settings corresponding to the different pattern sizes and search areas.

### 3. Results

In this study, we assess the performances of the MCC method in reproducing a known velocity field. A first

requirement for validating this method is that a velocity is indeed returned. Table 1 shows the area, averaged over all the settings, where no value is returned, as well as the average surface current speed in the model. In fact, the four seas can be grouped in two categories:

- the high-average-speed seas (North Sea and the Channel), which also have low areas where no value is returned (less than 10%);
- and the low-average-speed seas (Bay of Biscay and western Mediterranean Sea), which have large areas where no value is returned by the MCC method (often over 20%).

For the four seas, there is no large difference between the four periods, although in both the Bay of Biscay and the Mediterranean Sea the MCC method returns the fewest values in January.

We shall now assess for the two categories how the accuracy of the MCC method varies with different settings, for the four periods.

#### a. The most accurate setting for each sea

Tables 2–5 present for each sea, from north to south, and for each period, the mean percentage of the study area for which a velocity value is returned by the MCC, where

- the corresponding speed is within  $0.2 \text{ m s}^{-1}$  from the reference
- the corresponding direction is within  $45^\circ$  from the reference.

Such criteria, in a real-life situation, would indicate in which sector of the water to search for a rescue operation even with no prior knowledge of the velocity field.

For the North Sea (Table 2) and the Channel (Table 3), the individual settings corresponding to the maximum area with accurate velocities vary with the period and with the sea, yet common features are found. In particular the performances of the MCC method tend to

TABLE 1. For the four regions and for the four periods considered, the average speed of the reference model's hourly output over the studied week (top) and the percentage of the region where no value is returned by the MCC method, averaged over all the time steps and the different settings (bottom).

		North Sea	The Channel	Bay of Biscay	Mediterranean Sea
Avg speed ( $\text{m s}^{-1}$ )	21–27 Jan 2016	$0.39 \pm 0.19$	$0.68 \pm 0.26$	$0.20 \pm 0.10$	$0.18 \pm 0.11$
	21–27 Apr 2016	$0.37 \pm 0.18$	$0.64 \pm 0.26$	$0.18 \pm 0.08$	$0.21 \pm 0.10$
	21–27 Jul 2016	$0.43 \pm 0.19$	$0.68 \pm 0.27$	$0.25 \pm 0.09$	$0.22 \pm 0.09$
	21–27 Oct 2016	$0.33 \pm 0.16$	$0.50 \pm 0.22$	$0.18 \pm 0.07$	$0.20 \pm 0.09$
Avg no-value area (%)	21–27 Jan 2016	$8 \pm 6$	$5 \pm 5$	$28 \pm 22$	$46 \pm 26$
	21–27 Apr 2016	$10 \pm 9$	$6 \pm 6$	$18 \pm 18$	$28 \pm 26$
	21–27 Jul 2016	$9 \pm 5$	$6 \pm 6$	$16 \pm 16$	$21 \pm 21$
	21–27 Oct 2016	$9 \pm 9$	$7 \pm 7$	$21 \pm 21$	$35 \pm 25$

TABLE 2. For the North Sea area, where a velocity is returned by the MCC method, the percentage of this area where the error in speed  $< 0.2 \text{ m s}^{-1}$  and the error in direction  $< 45^\circ$  for each time resolution (rows) and setting (columns) for the four periods: 21–27 Jan 2016 (Jan), 21–27 Apr 2016 (Apr), 21–27 Jul 2016 (Jul), and 21–27 Oct 2016 (Oct). Bold font indicates the maximum percentage for each period.

Template size (km)		5			10			20		
Search window (km)		10	20	30	10	20	30	10	20	30
1 h	Jan, Apr	39 41	39 40	38 39	43 43	43 42	44 43	42 34	44 38	46 42
	Jul, Oct	42 41	39 39	38 40	44 43	44 45	45 44	43 43	41 45	43 47
2 h	Jan, Apr	65 67	63 66	64 64	66 69	65 69	63 67	69 71	67 68	65 67
	Jul, Oct	55 67	54 66	51 65	59 72	59 70	55 69	62 70	60 70	58 67
3 h	Jan, Apr	65 67	63 65	63 63	66 68	66 67	65 67	71 71	65 69	64 66
	Jul, Oct	59 71	56 70	52 68	64 75	64 72	61 71	68 74	64 73	65 70
4 h	Jan, Apr	66 66	66 65	66 63	69 71	69 69	67 68	71 74	68 69	69 68
	Jul, Oct	63 73	61 70	53 69	67 73	67 72	65 72	71 72	68 72	69 71
5 h	Jan, Apr	70 69	69 68	68 66	71 72	69 70	68 68	76 74	72 71	71 71
	Jul, Oct	60 78	60 75	56 75	71 78	69 77	65 76	71 79	71 78	70 77
6 h	Jan, Apr	74 83	76 82	76 79	78 86	78 85	79 83	<b>77 87</b>	75 84	75 84
	Jul, Oct	68 75	62 73	57 71	74 76	73 75	71 75	78 75	75 73	76 74
9 h	Jan, Apr	80 77	81 76	82 75	83 81	84 81	85 80	82 80	85 79	83 81
	Jul, Oct	74 81	70 82	63 80	80 84	78 84	78 84	<b>81 82</b>	80 83	79 83
12 h	Jan, Apr	83 51	82 46	79 39	86 65	87 57	87 56	86 60	86 62	<b>89 57</b>
	Jul, Oct	61 78	57 74	52 73	72 84	68 84	67 83	75 84	71 <b>89</b>	73 85

improve as the time interval between the SST “images” increases. For all periods, more than 50% of the area is accurate in the North Sea for a time interval larger than 2 h, and larger than 5 h in the Channel. More than 66% of the area is accurate over 4 h in the North Sea, and over 9 h in the Channel. In both seas, the largest values are encountered for a time resolution between 6 and 12 h, and for a template size of 20 km. For all four periods, in these strong current seas, the maximum area is large and exceeds 80% (values in bold font; Tables 2 and 3).

In the Bay of Biscay (Table 4) and western Mediterranean Sea (Table 5) in contrast, the area where

MCC-calculated currents and reference currents coincide is rather low. In the Bay of Biscay, although the maximum in January and April is encountered for a template size of 20 km and a time interval of 2 h (Table 4), for all periods the accuracy is increased and larger than 50% for a time interval larger than 3 h and for a template size smaller than 20 km. Only January, which is also the month when the fewest values are returned (Table 1), has an accuracy larger than 66%, for a time interval between 3 and 5 h. The results are even poorer in the Mediterranean Sea where only in October, for a template size of 5 km and a time interval between 2 and 9 h do we have an accurate area larger than

TABLE 3. As in Table 2, but for the Channel.

Template size (km)		5			10			20		
Search window (km)		10	20	30	10	20	30	10	20	30
1 h	Jan, Apr	40 44	38 42	37 40	40 42	40 42	39 41	35 38	35 35	35 35
	Jul, Oct	42 52	41 53	39 51	41 55	41 54	39 53	36 53	32 47	35 52
2 h	Jan, Apr	42 46	41 45	39 43	44 47	43 48	42 46	41 43	38 42	38 46
	Jul, Oct	45 58	45 57	43 53	47 56	47 58	46 55	42 54	40 50	40 50
3 h	Jan, Apr	42 47	43 47	45 45	44 48	44 48	44 46	44 48	41 43	40 46
	Jul, Oct	44 59	46 59	43 58	47 59	49 61	47 61	44 56	43 55	42 55
4 h	Jan, Apr	40 46	47 49	47 45	46 48	47 52	48 49	47 49	46 48	44 48
	Jul, Oct	42 62	47 61	45 60	46 62	50 64	49 61	45 57	44 56	46 59
5 h	Jan, Apr	40 46	50 52	50 51	46 50	50 54	51 55	48 53	48 49	50 51
	Jul, Oct	43 64	50 65	47 64	47 66	57 68	55 62	50 64	45 62	49 59
6 h	Jan, Apr	47 45	55 54	52 54	51 49	57 59	55 60	54 52	52 50	52 52
	Jul, Oct	44 69	52 71	53 71	51 68	59 73	61 71	52 66	55 64	59 68
9 h	Jan, Apr	76 74	77 73	78 68	78 78	80 77	80 78	71 75	71 71	<b>82 80</b>
	Jul, Oct	67 81	70 82	69 80	75 81	76 81	<b>80 81</b>	67 80	69 79	<b>75 84</b>
12 h	Jan, Apr	66 30	68 21	62 25	71 24	74 23	71 17	54 24	66 34	69 23
	Jul, Oct	50 59	50 60	47 60	55 62	52 59	50 58	50 60	45 53	50 59

TABLE 4. As in Table 2, but for the Bay of Biscay.

Template size (km)		5			10			20		
Search window (km)		10	20	30	10	20	30	10	20	30
1 h	Jan, Apr	35 33	21 21	15 11	40 39	28 20	22 9	20 0	14 0	20 0
	Jul, Oct	21 13	17 8	16 9	28 4	21 0	17 10	13 0	0 0	19 0
2 h	Jan, Apr	61 55	62 51	57 47	64 60	68 60	67 59	67 <b>67</b>	<b>71</b> 65	70 60
	Jul, Oct	43 47	42 46	41 45	40 42	40 41	39 40	35 41	38 40	37 36
3 h	Jan, Apr	69 63	66 57	66 54	70 63	70 61	70 63	69 66	<b>71</b> 60	69 63
	Jul, Oct	50 55	48 54	43 52	45 49	46 49	48 51	40 45	42 45	42 44
4 h	Jan, Apr	69 62	66 59	67 54	69 62	68 62	68 60	64 59	67 57	63 58
	Jul, Oct	52 60	48 57	43 56	50 56	50 56	49 56	44 47	44 46	46 46
5 h	Jan, Apr	71 61	69 57	67 53	67 59	67 60	68 58	64 54	67 54	64 54
	Jul, Oct	52 62	48 60	42 57	51 56	48 58	48 59	44 48	48 48	47 49
6 h	Jan, Apr	67 61	65 55	64 50	63 59	64 58	63 57	63 55	63 53	61 53
	Jul, Oct	54 63	48 60	42 58	51 59	50 59	48 60	47 52	49 51	49 50
9 h	Jan, Apr	63 54	59 48	59 46	59 54	58 52	59 48	53 46	54 48	55 45
	Jul, Oct	<b>57</b> 63	53 61	43 58	56 57	55 60	53 60	50 52	49 51	49 52
12 h	Jan, Apr	53 50	53 46	46 41	51 47	51 47	49 46	39 41	45 43	36 42
	Jul, Oct	53 <b>64</b>	48 60	43 61	54 60	52 62	51 62	47 54	45 50	45 57

50%. For both seas, as long as the time interval is larger than 1 h, there is no large seasonal difference.

In summary, strong currents (in the North Sea and the Channel) are more accurately retrieved for a large template size (20 km) and time interval (9 h; Tables 2 and 3). This is consistent with Matthews and Emery (2009), who used a template size of 24 km to retrieve the mean strong California Coastal Current, and Bowen et al. (2002), who used 30 km for the east Australian coastal current. The large time interval probably allows for a wider range of velocities to be accurately retrieved. For the weak currents in contrast (in the Bay of Biscay and the western Mediterranean Sea), a lower template size (5 or 10 km) and time

interval (3–6 h; Tables 4 and 5) return the most accurate results. This is consistent with Warren et al. (2016), who used a 10-km template size to retrieve the low velocities ( $0.12\text{--}0.25\text{ m s}^{-1}$ ) of the Korea Strait. Heuzé et al. (2017) in particular found that a small time interval was necessary in the Mediterranean Sea because of the presence of many eddies, which destroy the temperature patterns that the MCC method is designed to track. In all regions, the size of the search window did not seem to significantly impact the results, nor did the different periods.

This assessment was based on criteria that take into account both components of the velocity at the same time, but maybe, as a result of the geometry of each sea,

TABLE 5. As in Table 2, but for the western Mediterranean Sea.

Template size (km)		5			10			20		
Search window (km)		10	20	30	10	20	30	10	20	30
1 h	Jan, Apr	0 24	0 27	4 22	34 19	13 23	20 17	0 0	0 0	0 0
	Jul, Oct	15 14	17 15	17 10	0 0	0 0	11 0	0 0	0 0	0 0
2 h	Jan, Apr	32 40	35 39	35 36	23 35	18 35	16 32	16 17	0 17	16 15
	Jul, Oct	45 54	45 53	44 53	39 47	40 48	41 47	26 25	25 34	23 42
3 h	Jan, Apr	40 <b>46</b>	40 44	40 40	34 39	32 39	32 39	27 27	20 26	20 25
	Jul, Oct	49 <b>56</b>	48 54	46 52	45 48	45 49	44 48	32 39	29 40	30 42
4 h	Jan, Apr	44 45	42 44	42 42	37 41	37 41	35 41	25 29	21 27	21 26
	Jul, Oct	<b>50</b> 55	48 53	44 52	47 50	47 49	45 49	35 37	33 36	32 39
5 h	Jan, Apr	<b>45</b> 45	43 43	41 40	39 42	39 41	39 40	31 33	24 29	27 28
	Jul, Oct	<b>50</b> 55	47 54	44 52	48 49	47 48	45 48	35 33	32 34	33 35
6 h	Jan, Apr	44 45	43 42	42 41	39 43	39 42	39 41	32 33	25 32	25 30
	Jul, Oct	49 <b>56</b>	46 53	43 52	48 50	45 49	43 50	35 34	32 37	34 36
9 h	Jan, Apr	44 44	43 42	42 37	41 42	41 40	42 40	31 33	26 28	26 29
	Jul, Oct	45 55	42 52	38 50	46 51	44 50	43 49	35 34	32 36	33 33
12 h	Jan, Apr	<b>45</b> 40	42 35	40 35	44 40	42 38	42 36	27 32	24 29	26 29
	Jul, Oct	44 51	41 49	37 45	44 48	43 48	42 49	33 32	35 31	30 33



one component is easier to retrieve than the other? This is the topic of the next section.

### *b. Zonal versus meridional component accuracy*

Since the accuracy of the MCC method does not seem to be season dependent in this study, we now concentrate on only one of the periods. We choose 21–27 October 2016, which is not an extreme in velocity for any of the regions (Table 1). Figures 2 and 3 show the performance of each setting in the four seas, for the two velocity components  $u$  (gray color scale) and  $v$  (warm color scale) separately using Taylor diagrams, for four selected time intervals (2, 4, 6, and 9 h). The 12-h setting was discarded, since it is not performing better than 9 h in the previous section, and it has the lowest number of time steps (14). The focus in this section is not to determine which setting is the best, but whether one setting performs significantly better than the others, and whether there is a strong difference between  $u$  and  $v$ . With this type of representation, the most accurate setting is the one whose dot is closest to its reference (Taylor 2001).

For all seas, the range of standard deviation decreases as the time interval increases (Figs. 2 and 3, compared from top to bottom). This is probably because brief, extreme values are smoothed by the long-time averaging. The correlations are relatively similar for all time intervals of each sea though, suggesting that the model's surface velocity (the reference) and sea surface temperature have the same dynamics, at least at the temporal scales considered in this study. This would not be true for times larger than 12 h, that is, when horizontal diffusion, local cooling or heating, and vertical mixing are no longer negligible compared to advection (Tokmakian et al. 1990).

In the North Sea at low time intervals (Fig. 2a), the zonal component ( $u$ , gray) has too large a standard deviation and a lower correlation than the meridional component ( $v$ , warm) when compared to the reference. The standard deviation of  $u$  decreases as the time interval increases, whereas that of  $v$  does not change significantly. Similarly, in the Channel (Fig. 2, right), for low time intervals, the standard deviation of  $u$  is larger than twice that of the reference and hence its points are off the chart (Figs. 2e and 2f). Besides, for  $v$  all settings perform similarly, but for  $u$ , the three settings with a search area of 10 km (circle symbols) outperform the other settings. As in section 3a, we find that these two seas with strong currents have the most accurate retrievals for large time intervals.

Moreover in the Channel, a small search area leads to an increased accuracy of the retrieved zonal velocity. This is probably because the zonal SST

gradient is very weak in the Channel over the period 21–27 October 2016 [ $0.02^{\circ}\text{C} (\text{°longitude})^{-1}$ ], 5 times weaker than the meridional SST gradient, and an order of magnitude smaller than in the North Sea. As a result, the MCC algorithm can fail to distinguish SST patterns and return spurious high velocities, corresponding to unrealistic correlations between the east and west parts of the basin. A small search radius then constrains the velocities and limits their maximum value.

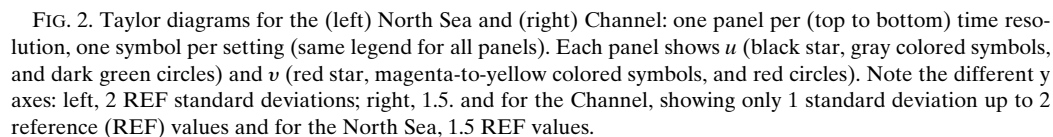
In the Bay of Biscay (Fig. 3, left), in agreement with Table 4, the accuracy of both  $u$  and  $v$  is best for the time intervals 4 and 6 h. No setting seems significantly better than the others, and the majority of settings have a correlation lower than in the North Sea and Channel. Similarly in the Mediterranean Sea (Fig. 3, right), the correlation rarely exceeds 0.7. As in Table 5, the 4-h time interval and 5-km template size (small black and magenta symbols) setting returns significantly better results than the others for  $u$  and  $v$  in the Mediterranean Sea.

In summary, apart from the Channel, which has a weak zonal SST gradient, there is no clear difference between the accuracy of the zonal and meridional components of the velocity. For the North Sea and the Channel (Fig. 2), no setting is particularly inaccurate. The accuracy is less in the Bay of Biscay and the Mediterranean Sea (Fig. 3). In fact, only in the Mediterranean Sea did one setting clearly perform better than the others, and this setting is not the same as was found using Table 5. So what caused the differences in Tables 2–5? We now check to see whether that could be the strength of the current itself.

### *c. Better if faster, stronger*

Studies that aim at retrieving surface currents from SST usually concentrate on a small region and conclude that their result is probably region or current dependent (e.g., Emery et al. 1986; Tokmakian et al. 1990; Bowen et al. 2002; Doronzo et al. 2015). We verify this assumption here by looking at four different regions. Figure 4 shows for each region, of all the time steps of their respective setting with the largest number of accurate points returned (Tables 1–5), the one that is most accurate when comparing the original model velocities (left) to the ones retrieved (right).

In fact, the most striking feature is the amount of points where a velocity is not retrieved (white areas in Fig. 4). As was already shown by Table 1, in the North Sea and in the Channel (Figs. 4a and 4b, respectively), this number is relatively low and is mostly limited to the coastal regions that we purposely excluded from our algorithm. In the Bay of Biscay however (Fig. 4c) and





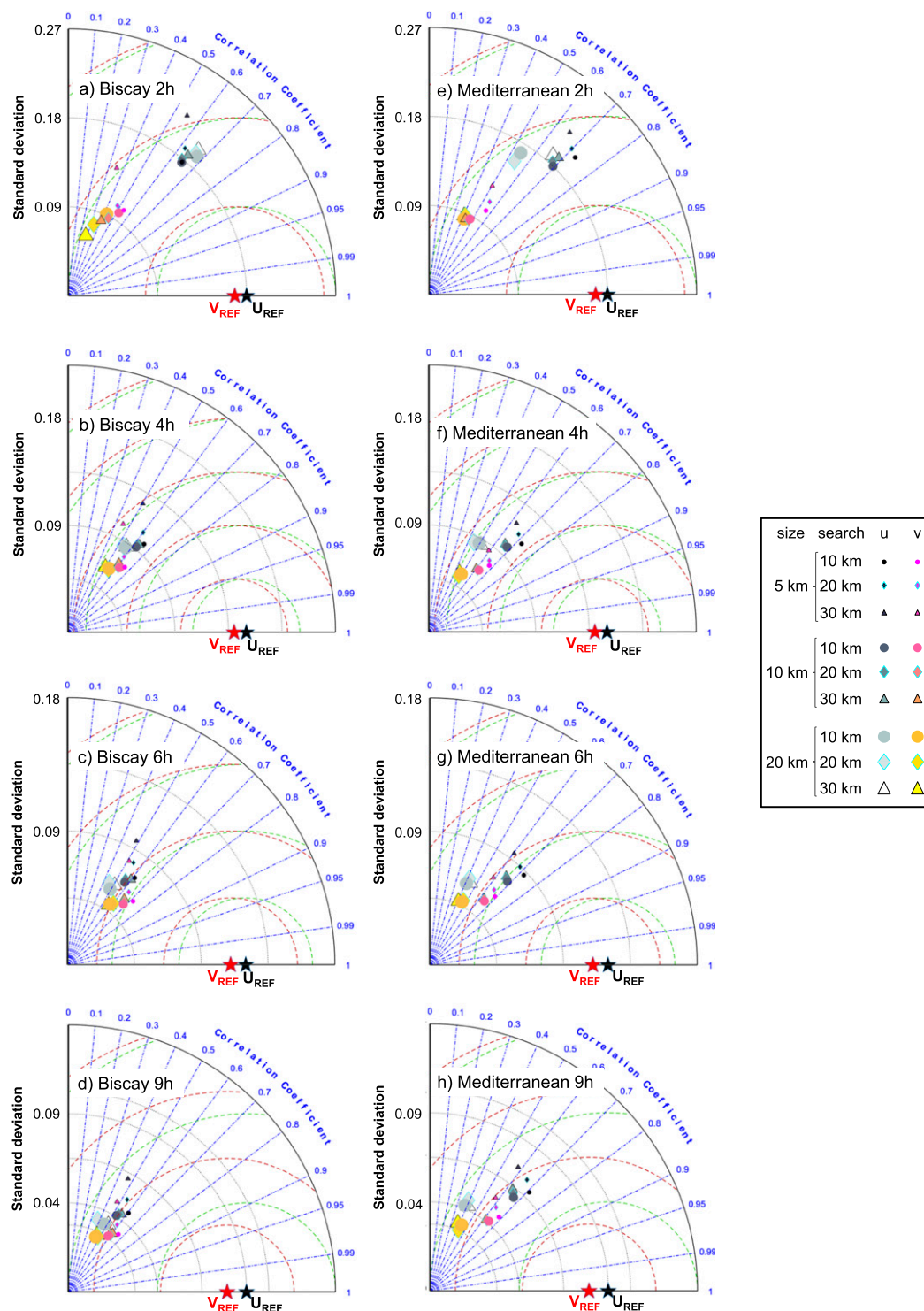


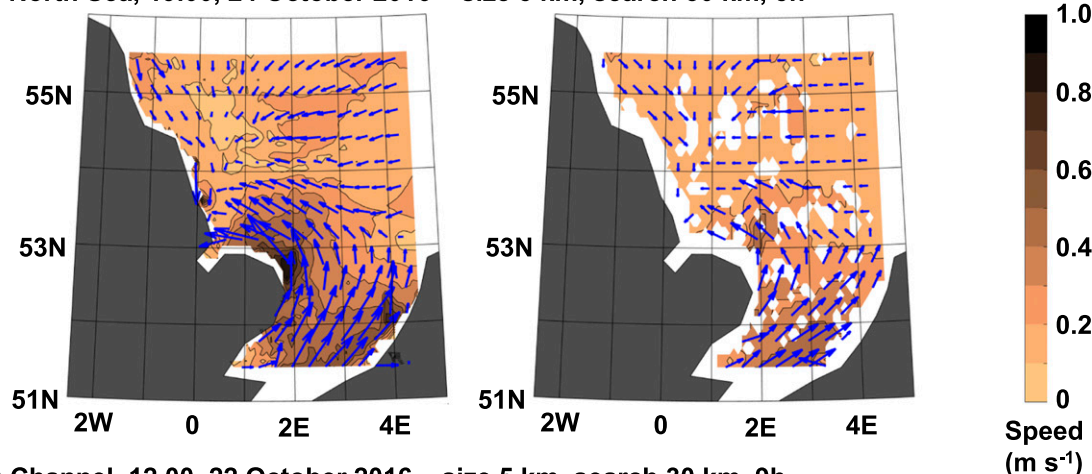
FIG. 3. As in Fig. 2, but for (left) the Bay of Biscay and (right) the western Mediterranean Sea.

even more in the western Mediterranean (Fig. 4d), there are many nonreturned points in areas with low velocities (dark blue). This is consistent with many studies, from Emery et al. (1986) to Heuzé et al. (2017), which showed

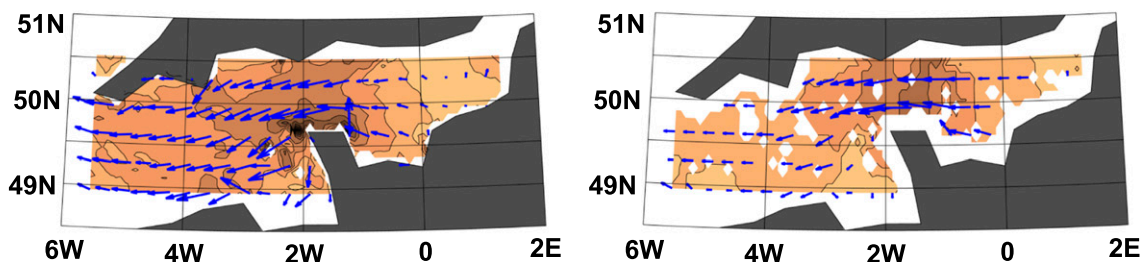
that the MCC method cannot work if the temperature patterns do not move much during the time interval.

For all seas, both the velocity and the direction are correctly reproduced, even in the seemingly more

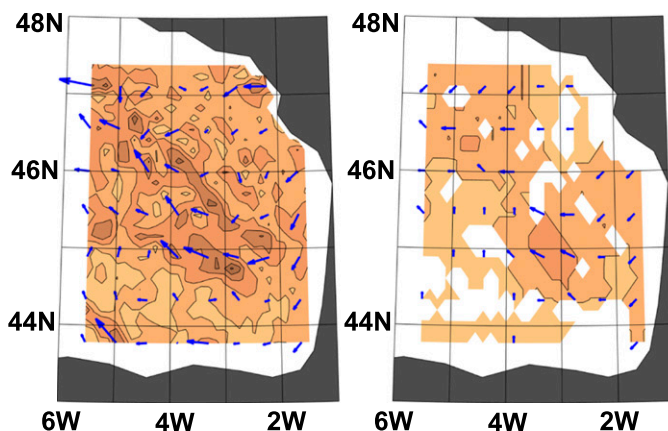
a) North Sea, 19.00, 24 October 2016 – size 5 km, search 30 km, 5h



b) Channel, 12.00, 22 October 2016 – size 5 km, search 30 km, 9h



c) Bay of Biscay, 12.00, 26 October 2016 – size 10 km, search 30 km, 6h



d) Mediterranean Sea, 9.00, 21 October 2016 – size 5 km, search 20 km, 9h

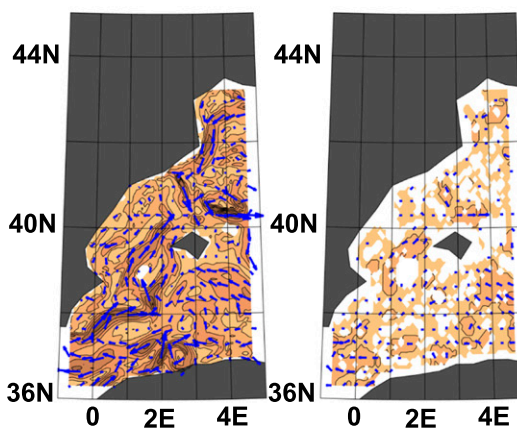


FIG. 4. A comparison between the (left) reference and (right) retrieved velocities for the (a)–(d) four regions of this study for their settings with the largest amount of accurate points returned. The same scale is used for all the panels. The number of wind arrows is decreased by four in latitude and longitude for clarity.

complex areas. In the North Sea, for example, the current accurately turns westward north of 53°N to follow the English coast (Fig. 4a). In the Channel, both the reference and retrieved currents are strongest around 2°W and dip southward as they flow westward (Fig. 4b). Even in the complex swirling Mediterranean Sea,

when a direction is returned it is relatively accurate (Fig. 4d).

In fact, in our study, the accuracy is not location specific. For all the seas, the velocities returned are accurate. It is the number of these velocities that are returned that depends on the location. If the region has

low velocities, as is the case in this study for the Bay of Biscay and the Mediterranean Sea (Figs. 4c and 4d), then a very large time interval between two images becomes necessary to retrieve more velocity value. But over 12 h, the assumption that the sea surface temperature is purely advected is not valid anymore (Tokmakian et al. 1990) and the MCC method can no longer be used.

#### 4. Conclusions

In this paper, we compared the sea surface current velocities from a model with the current velocities retrieved by applying the maximum cross-correlation method to the sea surface temperature of the same model. The aims of this study were as follows:

- to validate this cross-correlation method using a known velocity field from a model as a reference in order to see which biases are introduced by the algorithm;
- to perform a sensitivity study in order to determine the best settings when applying this method, using the model output as a reference;
- to compare the results over four different periods and four different seas in order to assess whether our results are region specific.

The biases induced by applying this algorithm—that is, the differences between the known model field and the retrieved field—are lower than  $0.2 \text{ m s}^{-1}$  in speed and  $45^\circ$  in direction for retrievals separated by only a few hours. We have thus shown that this algorithm is accurate enough and could theoretically be used operationally on actual spaceborne sea surface temperature data (e.g., to determine a search area for search and rescue operations; Davidson et al. 2009). The results in this study are not region specific, but in regions with low velocities the algorithm can less often retrieve values: the values retrieved are accurate, but there are fewer of them.

We found that the highest accuracy was obtained for all regions for a time interval between two images of 4–9 h. This is compatible with already-existing satellite technology. In fact, Advanced Very High Resolution Radiometer images have an even higher horizontal resolution than the model used in this study (1 km), and since this instrument is aboard several satellites, images can be obtained every 2–6 h. Our study suggests that automated near-real-time retrieval of sea surface currents from AVHRR sea surface temperature is possible to implement.

One limitation though is that the presence of clouds can reduce the number of available images. The MCC

method also assumes that the current is purely advected and would probably struggle in frontal zones and eddy-rich areas. Yet, for the confinement of an oil spill, search and rescue missions, open ocean navigation fuel efficiency, or even the historical variability of mean currents, retrieving the surface currents from sea surface temperature seems to be an accurate and effective solution.

**Acknowledgments.** This work was funded by the Swedish National Space Board (Dnr. 167/14). CH is funded by a VINNOVA Marie Curie fellowship (Dnr. 2015-01487). The authors thank the two anonymous reviewers, whose comments notably increased the robustness and clarity of the manuscript. CH would like to thank Guillaume Ducrozet and Yves Perignon from École Centrale de Nantes for suggesting the model used in this study.

#### REFERENCES

- Bowen, M. M., W. J. Emery, J. L. Wilkin, P. C. Tildesley, I. J. Barton, and R. Knewton, 2002: Extracting multiyear surface currents from sequential thermal imagery using the maximum cross-correlation technique. *J. Atmos. Oceanic Technol.*, **19**, 1665–1676, doi:10.1175/1520-0426(2002)019<1665:EMSCFS>2.0.CO;2.
- Davidson, F. J. M., and Coauthors, 2009: Applications of GODAE ocean current forecasts to search and rescue and ship routing. *Oceanography*, **22**, 176–181, doi:10.5670/oceanog.2009.76.
- Doronzio, B., S. Taddei, C. Brandini, and M. Fattorini, 2015: Extensive analysis of potentialities and limitations of a maximum cross-correlation technique for surface circulation by using realistic ocean model simulations. *Ocean Dyn.*, **65**, 1183–1198, doi:10.1007/s10236-015-0859-1.
- Emery, W. J., A. C. Thomas, M. J. Collins, W. R. Crawford, and D. L. Mackas, 1986: An objective method for computing advective surface velocities from sequential infrared satellite images. *J. Geophys. Res.*, **91**, 12 865–12 878, doi:10.1029/JC091iC11p12865.
- , C. Fowler, and C. A. Clayson, 1992: Satellite-image-derived Gulf Stream currents compared with numerical model results. *J. Atmos. Oceanic Technol.*, **9**, 286–304, doi:10.1175/1520-0426(1992)009<0286:SIDGSC>2.0.CO;2.
- Heuzé, C., G. Caravajal, L. Eriksson, and M. Soja-Woźniak, 2017: Sea surface currents estimated from spaceborne infrared images validated against reanalysis data and drifters in the Mediterranean Sea. *Remote Sens.*, **9**, 422, doi:10.3390/rs9050422.
- Klemas, V., 2012: Remote sensing of coastal and ocean currents: An overview. *J. Coastal Res.*, **28**, 576–586, doi:10.2112/JCOASTRES-D-11-00197.1.
- Madec, G., 2008: NEMO ocean general circulation model reference manual. LODYC/IPSL Tech. Rep., 27 pp.
- Marcello, J., F. Eugénion, F. Marques, A. Hernandez-Guerra, and A. Gasull, 2008: Motion estimation techniques to automatically track oceanographic thermal structures in multisensor

- image sequences. *IEEE Trans. Geosci. Remote Sens.*, **46**, 2743–2762, doi:[10.1109/TGRS.2008.919274](https://doi.org/10.1109/TGRS.2008.919274).
- Matthews, D., and W. Emery, 2009: Velocity observations of the California Current derived from satellite imagery. *J. Geophys. Res.*, **114**, C08001, doi:[10.1029/2008JC005029](https://doi.org/10.1029/2008JC005029).
- Pascual, A., M.-I. Pujol, G. Larnicol, P.-Y. Le Traon, and M.-H. Rio, 2007: Mesoscale mapping capabilities of multisatellite altimeter missions: First results with real data in the Mediterranean Sea. *J. Mar. Syst.*, **65**, 190–211, doi:[10.1016/j.jmarsys.2004.12.004](https://doi.org/10.1016/j.jmarsys.2004.12.004).
- Ronen, D., 2011: The effect of oil price on containership speed and fleet size. *J. Oper. Res. Soc.*, **62**, 211–216, doi:[10.1057/jors.2009.169](https://doi.org/10.1057/jors.2009.169).
- Shchepetkin, A. F., and J. C. McWilliams, 2005: The regional ocean modeling system: A split-explicit, free-surface, topography-following-coordinate oceanic model. *Ocean Modell.*, **9**, 347–404, doi:[10.1016/j.ocemod.2004.08.002](https://doi.org/10.1016/j.ocemod.2004.08.002).
- Simpson, J. J., and J. I. Gobat, 1994: Robust velocity estimates, stream functions, and simulated Lagrangian drifters from sequential spacecraft data. *IEEE Trans. Geosci. Remote Sens.*, **32**, 479–493, doi:[10.1109/36.297966](https://doi.org/10.1109/36.297966).
- Sotillo, M. G., and Coauthors, 2015: The MyOcean IBI Ocean Forecast and Reanalysis Systems: Operational products and roadmap to the future Copernicus Service. *J. Oper. Oceanogr.*, **8**, 63–79, doi:[10.1080/1755876X.2015.1014663](https://doi.org/10.1080/1755876X.2015.1014663).
- Stewart, R. H., and J. W. Joy, 1974: HF radio measurements of surface currents. *Deep-Sea Res. Oceanogr. Abstr.*, **21**, 1039–1049, doi:[10.1016/0011-7471\(74\)90066-7](https://doi.org/10.1016/0011-7471(74)90066-7).
- Taylor, K. E., 2001: Summarizing multiple aspects of model performance in a single diagram. *J. Geophys. Res.*, **106**, 7183–7192, doi:[10.1029/2000JD900719](https://doi.org/10.1029/2000JD900719).
- Tokmakian, R., P. T. Strub, and J. McClean-Padman, 1990: Evaluation of the maximum cross-correlation method of estimating sea surface velocities from sequential satellite images. *J. Atmos. Oceanic Technol.*, **7**, 852–865, doi:[10.1175/1520-0426\(1990\)007<0852:EOTMCC>2.0.CO;2](https://doi.org/10.1175/1520-0426(1990)007<0852:EOTMCC>2.0.CO;2).
- Wahl, D. D., and J. J. Simpson, 1990: Physical processes affecting the objective determination of near-surface velocity from satellite data. *J. Geophys. Res.*, **95**, 13 511–13 528, doi:[10.1029/JC095iC08p13511](https://doi.org/10.1029/JC095iC08p13511).
- Warren, M. A., G. D. Quartly, J. D. Shutler, P. I. Miller, and Y. Yoshikawa, 2016: Estimation of ocean surface currents from maximum cross correlation applied to GOCI geostationary satellite remote sensing data over the Tsushima (Korea) Straits. *J. Geophys. Res. Oceans*, **121**, 6993–7009, doi:[10.1002/2016JC011814](https://doi.org/10.1002/2016JC011814).